scientific reports

Check for updates

OPEN

Suzi Daotan Decoction alleviates asthmatic airway remodeling through the AMPK/SIRT1/PGC-1α signaling pathway and PI3K/AKT signaling pathway

Kaiyue Liu[1,2,7], Ruobai Liu[1,3,7], Chenghao Zhang[1,4,7], Dandan Huang[1,2], Bowen Wei[1,2], Yilan Song[1,3], Chongyang Wang[1,3], Xin Zhang[6], Mingyu Zheng[1,2,5]✉ & Guanghai Yan[1,3,5]✉

Suzi Daotan Decoction (SZDTD), recorded in the "New Edition of the Sasang of Eastern Medicine", serves as a prominent formula for managing asthma in Shao-Yin individuals in Korean traditional medicine. This prescription demonstrates clinical efficacy in asthma treatment and is associated with anti-inflammatory and antioxidant properties. Nonetheless, the precise underlying mechanism remains incompletely understood. This study aims to elucidate the impact of SZDTD in ameliorating asthmatic airway remodeling and investigate whether its mechanism is related to the AMPK/SIRT1/PGC-1α and PI3K/AKT signaling pathways. Through network pharmacology analysis, the components and putative targets of SZDTD were investigated, along with the target genes associated with allergic asthma. Enrichment analysis identified the AMPK/SIRT1/PGC-1α and PI3K/AKT signaling pathways as relevant pathways. Subsequently, in an allergic asthma mouse model sensitized and challenged with ovalbumin (OVA), mice were orally administered a low dose of SZDTD, a high dose of SZDTD, or dexamethasone before the challenge. The control group received 0.9% NaCl only. The number of inflammatory cells was assessed using Diff-Quik staining. The levels of interleukin-4(IL-4), IL-5, IL-13 in broncho-alveolar lavage fluid (BALF), total immunoglobulin E(IgE), and OVA-specific IgE in serum were detected by Enzyme-linked immunosorbent assay. IL-4 and interferon γ (IFN-γ) in spleen and lymph were detected by flow cytometry. Histological staining was employed to observe lung tissue pathology. Protein levels were evaluated using Immunohistochemistry(IHC), Western blotting (WB), and immunofluorescence (IF). Furthermore, BEAS-2B human bronchial epithelial cells stimulated with LPS were treated with varying concentrations of SZDTD, and WB analysis was conducted to determine associated protein levels. SZDTD demonstrated a significant reduction in inflammatory cell infiltration, as well as decreased levels of IL-4, IL-5, and IL-13 in BALF, and total IgE and ovalbumin-specific IgE levels in serum. Flow cytometry analysis revealed that SZDTD treatment led to decreased levels of IFN-γ and IL-4 in the lymph nodes and spleen, with a more pronounced effect observed on IL-4 level. Moreover, results from MASSON staining indicated that SZDTD treatment markedly reduced the expression of α-SMA (α-smooth muscle actin) and mitigated collagen deposition symptoms. Furthermore, SZDTD stimulated the phosphorylation of Adenosine 5′-monophosphate-activated protein kinase (AMPK) and enhanced the expression of Silent information regulator 1 (SIRT1) and Peroxisome proliferator-activated receptor gamma coactivator 1α (PGC-1α), while inhibiting the expression of P-PI3K, P-AKT. In vitro experiments showed that SZDTD promoted the phosphorylation of AMPK, increased the expression of SIRT1 and PGC-1α, and suppressed the expression of P-PI3K, P-AKT. SZDTD can alleviate airway remodeling in allergic asthma by a mechanism related to activation of AMPK/SIRT1/PGC-1α and inhibition of PI3K/AKT signaling pathways.

[1]Jilin Key Laboratory for Immune and Targeting Research On Common Allergic Diseases, Yanbian University, Yanji 133002, Jilin, People's Republic of China. [2] Department of Integrated Chinese and Western Medicine, Yanbian University Medical College, No. 977, Gongyuan Road, Yanji 133002, Jilin Province, People's Republic of China. [3]Department of Anatomy, Histology and Embryology, Yanbian University Medical College, No. 977, Gongyuan Road, Yanji 133002, Jilin Province, People's Republic of China. [4]Department of Oral Teaching and Research, Yanbian

University Medical College, Yanji 133000, Jilin Province, China. [5]Key Laboratory of Natural Medicines of the Changbai Mountain, Ministry of Education, Yanbian University, Yanji 133002, People's Republic of China. [6]Changbai Mountain Protection Development Zone Central Hospital, Antu 133600, People's Republic of China. [7]Kaiyue Liu, Ruobai Liu and Chenghao Zhang contributed equally to this work. ✉email: myzheng@ybu.edu.cn; ghyan2015@sina.com; ghyan@ybu.edu.cn

Asthma, a chronic condition impacting the lung airways, has been identified by the World Health Organization as one of the top three diseases to focus on in the twenty-first century. Symptoms of asthma include breathing difficulties arising from variable airway obstruction and increased airway responsiveness, which are hallmark features of the condition[1,2]. Nowadays, with the continuous development of society, the prevalence of asthma is increasing and asthma accounted for 60,000 Disability-adjusted life year (DALY) globally in 2019, encompassing an estimated 26.2 billion (4.224–1.309) prevalent cases and 370,000 (0.29–6.45) new cases. The prevalence of chronic respiratory diseases greatly influences the annual incidence of epidemic diseases[3]. Allergic asthma, as the most common phenotype of asthma, usually begins in childhood and may persist throughout life. Airway remodeling refers to structural changes in the airway wall, including extensive epithelial damage, airway smooth muscle (ASM) hypertrophy and hyperplasia, collagen deposition, and fibrosis[4]. Airway remodeling is a decisive factor in the natural course of asthma and serves as a fundamental pathological characteristic of the condition[5].

As a branch of Traditional Chinese Medicine (TCM), Korean Medicine has a hundred years of experience in asthma management. SZDTD represents a traditional Korean Medicine prescription renowned for its notable efficacy in treating asthma in individuals with Shao-Yin constitution. A previous study has demonstrated that SZDTD may alleviate asthma through the WNT5A signaling pathway[6]. However, the specific mechanism was not deeply investigated. This study aims to investigate the mechanism of SZDTD in relation to allergic asthma through network pharmacology and subsequently validate it through experiments. The objective is to elucidate the mode of action of SZDTD for enhanced utilization and to offer insights for the development of novel therapeutics.

Material and methods

Gene networks analysis

The chemical composition data for the compound formula was obtained utilizing the Traditional Chinese Medicine Synthesis Database (TCMSP, https://tcmspw.com/tcmsp.php)[7]. The chemical constituents of each of the eight Chinese medicines comprising the SZDTD were investigated through this database: Perillae fructus (ZSZ, Zisuzi in Chinese; specimen deposited in National Institutes for Food and Drug Control, YD-132), Pinelliae rhizome (BX, Banxia in Chinese; specimen deposited in National Institutes for Food and Drug Control, YD-048), Angelicae sinensis radix (DG, Danggui in Chinese; specimen deposited in National Institutes for Food and Drug Control, YD-050), Arisaematis rhizomao (TNX, Tiannanxing in Chinese; specimen deposited in Guangdong Institute for Drug Control, 10500210001), Citrireticulatae pericarpium (CP, Chenpi in Chinese; specimen deposited in National Institutes for Food and Drug Control, YD-069), Magnoliae officinalis cortex (HP, Houpu in Chinese; specimen deposited in Gansu Institute for Drug Control, 10403550007), Aurantii fructus immaturus (ZS, Zhishi in Chinese; specimen deposited in National Institutes for Food and Drug Control, YD-086), and Glycyrrhizae radix et rhizome (GC, Gancao in Chinese specimen deposited in Gansu Institute for Drug Control, 10400410026). The filtering conditions were drug-likeness (DL) ≥ 0.18 and oral bioavailability (OB) ≥ 30%[8]. The chemical constituents of eight herbal medicines were also searched using the herb database (http://herb.ac.cn/)[9] and entered into the Pubchem database (https://pubchem.ncbi.nlm.nih.gov/)[10] to screen the active ingredients according to Lipinski's five principles[11]. The primary active components of SZDTD were identified by combining and de-weighting the active compounds obtained from the two databases. The Canonical SMILES chemical formula of each component was obtained from PubChem. Subsequently, the chemical formulas were input into the Swiss Target Prediction platform (http://swisstargetprediction.ch/) to identify their respective targets with a probability threshold > 0.3[12]. Following this, allergic asthma target predictions (Genecards, score of 1 or more; DisGeNET, score ≥ 0) were conducted using databases such as OMIM database (https://omim.org/), Genecards database (https://www.genecards.org/), Therapeutic Target Database(https://db.idrblab.net/ttd/), Drugbank (https://go.drugbank.com/), and DisGeNET (https://www.disgenet.org/)[13]. Potential targets of SZDTD for the treatment of allergic asthma were identified as the intersection of illness targets and targets of herbal components. To ensure standardization, the predicted targets were mapped to the UniProt database (https://www.uniprot.org/). The above two targets were imported into the Venn diagram tool (http://bioinformatics.psb.ugent.be/webtools/Venn/) to take the intersection, yielding the final target utilized for the mechanistic action of the SZDTD components. A protein–protein interaction (PPI) network was constructed and analyzed using a STRING (Version11.5, https://string-db.org/)[14] and Cytoscape software (Version 3.9.1; http://www.cytoscape.org)[15] to elucidate the molecular mechanisms underlying the asthma-relieving effects of SZDTD. The key points were analyzed using the DAVID platform (https://david.ncifcrf.gov/)[16] for the gene ontology (GO) function and Kyoto Encyclopedia of Genes and Genomes (KEGG) pathway enrichment analysis.

Preparation of SZDTD

The drugs utilized in the in vivo experiments comprised SZDTD consisting of the following herbal components: ZSZ (10 g), BX (7.5 g), DG (7.5 g), TNX (5 g), CP (5 g), HP (3.5 g), ZS (3.5 g), and GC (2.5 g), totaling 10 treatments. These herbal ingredients were sourced from Peking Tongrentang in Yanji City, China. The drug preparation was conducted using the aqueous extraction method. Following the completion of extraction, the liquid was stored in a refrigerator at 4°C. Following the completion of extraction for cellular experiments, the supernatant was dried under vacuum to yield a powder of 16.81%. The resulting extract was pulverized into a

powder and stored in a sealed container at 4 °C. This extraction method was technically supported by the College of Pharmacy, Yanbian University.

High performance liquid chromatography-mass spectrometry (HPLC–MS) analysis

Weigh 100 mg of thoroughly mixed samples into a 2 mL centrifuge tube. Add 1 mL of 70% methanol (Merck KGaA, Darmstadt, Germany) and 3 mm steel beads, and agitate the sample for 10 min using an automated sample homogenizer (JXFSTPRP-48, 70 Hz, JIngxin, Shanghai, China) for 3 min to facilitate breakdown. Subsequently, cool the sample, sonicate it at low temperature (40 kHz) for 10 min, then centrifuge for 10 min at 4 °C (12,000 rpm). Dilute the supernatant 2–100 times and combine with 10 µL of 100 µg/mL internal standard. Finally, filter the mixture through a 0.22 µm PTFE filter head for analysis. The instrumental analysis platforms used are listed below: Liquid chromatography-mass spectrometry (LC–MS) (Thermo, Ultimate 3000LC, Q Exactive HF) equipped with a C18 column (Zorbax Eclipse C18 (1.8 µm*2.1*100 mm), Agilent Technologies Inc, California, USA). The chromatographic separation conditions included a column temperature of 30 °C, a flow rate of 0.3 mL/min, and mobile phase composition of A: water with 0.1% formic acid (Sia Reagent, Shandong, China) and B: pure acetonitrile (Merck KGaA, Darmstadt, Germany). The injection volume was 2 µL, and the autosampler temperature was maintained at 4 °C. In positive mode, the instrumental parameters were set as follows: heater temperature at 325 °C, sheath gas flow rate at 45 arb, auxiliary gas flow rate at 15 arb, purge gas flow rate at 1 arb, electrospray voltage at 3.5 kV, capillary temperature at 330 °C, and S-Lens RF Level at 55%. In negative mode, the parameters were as follows: heater temperature at 325 °C, sheath gas flow rate at 45 arb, auxiliary gas flow rate at 15 arb, purge gas flow rate at 1 arb, electrospray voltage at 3.5 kV, capillary temperature at 330 °C, and S-Lens RF Level at 55%.

Animals

A total of 50 Specific pathogen-free BALB/c mice, aged 6 weeks and weighing approximately 20 g, were purchased from Yanbian University Medical Center. All mice were housed in the specific pathogen-free condition with room temperature of 22 ± 2 °C, relative humidity between 50%-60%, and a 12-h light–dark cycle. This study was approved by the Institutional Animal Care and Use Committee of Yanbian University (IACUC Issue NO.YD20230711001).

Murine allergic asthma model and treatment

As shown in Fig. 1, following a one-week acclimatization period, the mice were randomly divided into five groups: the control group (CON), the model group (MOD), the SZDTD low-dose group (LOW), the SZDTD high-dose group (HIGH), and the dexamethasone group (DEX), with n = 10 in each group. Intraperitoneal sensitization was performed on days 1, 7, and 14 with 200 µL of OVA solution in the ratio of 1 mg Al(OH)3 (Thermo Fisher Scientific, 81 Wyman Street, Waltham, MA, USA), 10 µg OVA (Solarbio, Beijing, China), and 20 mL of 0.9%NaCl. Enhanced sensitization was carried out on day 15, where each mouse received a 200 µL intraperitoneal injection of the OVA solution. The CON group was replaced with 0.9% NaCl. On day 16, the MOD group, LOW group, HIGH group, and DEX group were excited by ultrasonic nebulization (AER-S-AS, TOW-INT TECH, Shanghai, China) with a 1% OVA solution configured with 100 mg of OVA and 10 mL of 0.9% NaCl solution every other day. Simultaneously, the SZDTD was started to be administered by oral gavage, with a concentration of 150 mg/kg in the low-dose group, 300 mg/kg in the high-dose group, and 0.5 mg/kg in the DEX group, each administered as a 200 µL dose once daily for a total of 8 weeks. 0.9% NaCl was used instead of oral gavage in CON group and MOD group[17,18]. Following the last challenge, mice were humanely euthanized by cervical dislocation under deep anesthesia for further analysis.

Tissue sampling

2 h after the last OVA challenge, mice were anesthetized with barbiturates (100 mg/kg), and blood was collected from the eyes, centrifuged to obtain the supernatant, and frozen for storage. After execution, the trachea was exposed, a small opening was cut, the cannula was left in place, and 1.0 mL of 0.9% NaCl was injected into the lungs through the cannula with a syringe. The fluid was slowly withdrawn back, applying gentle pressure to the chest cavity while withdrawing, and this process was repeated three times. Subsequently, the collected bronchoalveolar lavage fluid was processed for further analysis. The collected bronchopulmonary lavage washings were centrifuged at 4°C, 1500 r/min for 5 min, and the supernatant was taken and frozen at − 80°C for subsequent testing. The centrifuged sediment was used to make cell smears. The lungs were extracted from the exposed chest cavity, the left lung was fixed in 10% formaldehyde for subsequent pathological observation. The right lung was sectioned into pieces, placed in sterile tubes labeled with group identifiers, and put into -80℃ refrigerator for protein extraction. The spleen was extracted from the exposed abdominal cavity, sectioned into

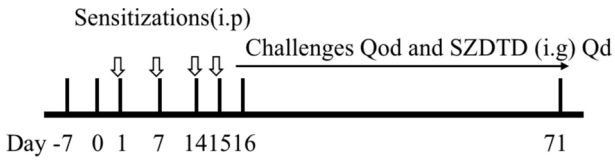

Fig. 1. Experimental protocol for allergic asthma mouse model. Sensitizations: 1 mg Al $(OH)_3$,10 µg OVA, 20 mL 0.9% NACL, Challenges: 1% OVA (100 mg OVA, 10 mL 0.9% NACL, n = 10).

pieces, and placed in a sterile tube labeled with a group identifier. The tube was then placed on ice. The cervical, axillary, and inguinal lymph nodes were also extracted, placed in a sterile tube containing 0.9% NaCl, labeled with a group identifier, and stored on ice.

Inflammatory factor count in broncho-alveolar lavage fluid (BALF).

After centrifugation, 1 mL of 0.9% NaCl was added to resuspend the remaining BALF precipitate. The cell suspension was coated with a flaker and then subjected to Diff-Quik (Solarbio, Beijing, China) rapid staining to differentiate the cell categories and counts in different fields of view.

Detection of cytokines in BALF and IgE in serum

Determination of cytokines IL-4 (BMS613, Invitrogen, USA), IL-5 (BMS610, Invitrogen, USA), IL-13 (KMC2221, Invitrogen, USA) in BALF and serum IgE and OVA-specific IgE (EMIGH, Invitrogen, USA) levels by ELISA according to the manufacturer's instructions.

Flow cytometry

Lymph nodes and spleens of each group were routinely isolated and processed to obtain a single-cell suspension. The cells were then stained with Percp-Cy5.5 CD3e (45-0031-80, Thermo Fisher Scientific, 81 Wyman Street, Waltham, MA, USA) and FITC-CD4 (35-0042-U100, MBL, Tokyo, Japan) following a 30-min incubation at 4°C in the dark. After washing and resuspending the cells in PBS, they were fixed, permeabilized, and subjected to an intracellular cytokine assay. Subsequently, PE-Cy7-IFN-γ (60-7311-U025, MBL, Tokyo, Japan) and APC-IL4 (20-7041-U100, MBL, Tokyo, Japan) were added for further analysis. Subsequently, the cells were washed, resuspended in PBS after 30 min of light protection at 4°C, and centrifuged to remove the supernatant. Next, the cells were treated with 4% paraformaldehyde and refrigerated at 4°C overnight.

Histopathological examination of lung tissues

The fixed lung tissues were paraffin-embedded and sectioned. Pathological sections were stained with Hematoxylin and Eosin staining (HE staining) and modified MASSON staining (Solarbio, Beijing, China) to observe the differences in the histopathological characteristics of each group. HE staining was used to evaluate the inflammation according to the infiltration of bronchial or peripheral inflammatory cells. MASSON staining was used to evaluate the airway remodeling.

Immunohistochemistry staining

The lung sections were placed in a 60 ℃ oven for melting wax, followed by a series of steps including dewaxing, dehydration, microwave heating, buffer cooling, and washing. Subsequently, the sections were incubated with the primary antibody, followed by the secondary antibody for the specific biomarkers, DAB (ZLI-9018, PV-9000, ZSGB-BIO, Beijing, China) chromatography, hematoxylin re-staining, dehydration, and finally, sealing of slices with neutral gum.

Immunofluorescence staining

The sections were subjected to a 60°C oven for wax melting, followed by sequential dewaxing, dehydration, antigen retrieval through microwave heating, and overnight incubation with primary antibodies. After washing, the sections were treated with a fluorescent secondary antibody, counterstained with DAPI for nuclear visualization. Subsequently, immunofluorescence was observed using a laser confocal microscope (Biotek Instruments, Inc.).

Western blot

The proteins were extracted, and their concentrations were determined using a BCA detection kit (#PC0020-500, Solarbio, Beijing, China). Subsequently, the proteins were separated on 10% SDS-PAGE gels and electrophoretically transferred onto PVDF membranes (Millipore, Billerica, MA, USA). Following blocking, the membranes were incubated overnight at 4°C with primary antibodies, and then with secondary antibodies at 37℃ for 1 h. Finally, the bands were developed with ECL (S0500, Millipore, USA), and scanned with AI600 Gel Imager (Bio-Tek, USA). Primary antibodies included AMPK (1:1250, #ab110036, Abcam, UK), SIRT1 (1:1000, #ab189494, Abcam, UK), PGC-1α (1:1500, #ab191838, Abcam, UK), α-SMA (1:1000, #19245, Cell Signaling Technology, USA), P-AMPK (1:1000, #44-1150G, Invitrogen, USA), and PI3K(1:1000, #MA1-74183, Invitrogen, USA), P-PI3K(1:1000, #PA5-104853 Invitrogen, USA), AKT (1:1000, #44-609G, Invitrogen, USA), P-AKT (1:2000, #4060S, Cell Signaling Technology, USA), β-actin (1:1000, #3700S,Cell Signaling Technology, USA). Secondary antibodies included goat anti-rabbit secondary antibody (1:11000, #ab6721, Abcam, UK) and anti-mouse secondary antibody (1:6000, #ab6789, Abcam, UK).

Cell culture and cell viability assay

The BEAS-2B human bronchial epithelial cell line was procured from the American Type Culture Collection in Rockville, Maryland, USA. These cells were cultured in Dulbecco's Modified Eagle Medium (DMEM) supplemented with 10% fetal bovine serum and 1% penicillin/streptomycin (both from Gibco BRL) under conditions of 37 ℃ and 5% CO_2. The culture medium was refreshed bi-daily, and cell passaging occurred every three to five days.

To assess the cytotoxic effects of various concentrations of SZDTD on BEAS-2B cells, doses of 12.5, 25, 50 μg/mL were tested. Additionally, to evaluate the impact of SZDTD on cell viability under simulated inflammatory conditions, BEAS-2B cells were pretreated with 10 ng/mL of lipopolysaccharide (LPS, Solarbio, Beijing, China) for 48 h. Subsequently, cell viability was measured using a 3-(4,5-dimethylthiazol-2-yl)-2,5-diphenyltetrazolium bromide (MTT) assay. For this assay, cells were seeded in a 96-well plate at a density of 1×10^4 cells per well.

Following a 72-h incubation, cells in five distinct groups were subjected to the respective treatments. After 24 h, the cells were stained with 20 μL of MTT solution for 4 h at 37 ℃. Subsequently, the medium was aspirated from each well, and the resultant purple formazan crystals were solubilized in 150 μL of dimethyl sulfoxide (DMSO) for 10 min. The absorbance was quantified at 490 nm using a microplate reader.

Consequently, the experimental groups were designated as follows: Control group (no drug treatment), LPS group (LPS only), LPS + SZDTD Low group, LPS + SZDTD Middle group, and LPS + SZDTD High group.

All methods were performed in accordance with the relevant guidelines and regulations.

Statistical analysis

All data analysis was performed with SPSS Version 20.0 (SPSS Inc.). The data were shown as mean ± SD. One-way analysis of variance (ANOVA) was used between multiple groups, two-way comparisons were made using the LSD test, $P < 0.05$ suggests significance. Statistical plots were drawn using GraphPad Prism 8.0.

Results

Identification and enrichment analysis of candidate targets for SZDTD against allergic asthma

The eight herbs in SZDTD have a total of 215 corresponding targets by database screening. In comparison, there were 2518 corresponding targets for allergic asthma, and a total of 86 common targets were identified (Fig. 2A). Subsequent network analysis of the shared targets, based on degree centrality, revealed that core genes such as AKT1, TNF, SRC, PTGS2, EGFR, PPADG, MMP9, ESR1, MMP2, and KDR were prominently involved (Fig. 2B, C; Table1).

The analysis of the 86 target genes through GO and KEGG enrichment revealed significant biological processes (BP) including response to xenobiotic stimulus, positive regulation of MAP kinase activity, positive regulation of vasoconstriction, positive regulation of smooth muscle cell proliferation, and extracellular matrix

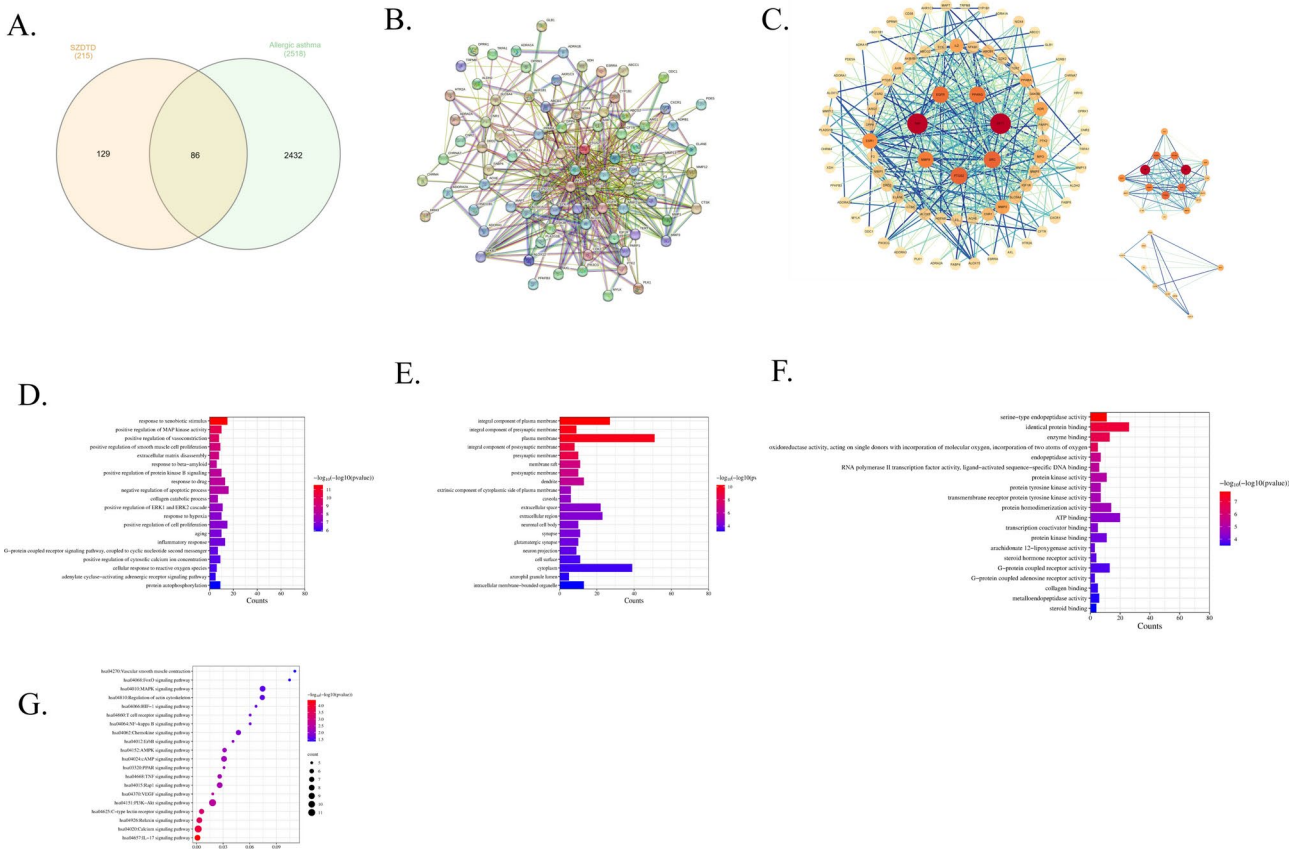

Fig. 2. Network Pharmacology analysis on the potential mechanisms of SZDTD against allergic asthma. (**A**) The Venn diagram demonstrates the number of intersected and specific targets between SZDTD and allergic asthma. (**B**) The interaction relationships of the intersecting targets were obtained through the STRING database. (**C**) Topological analysis of the protein–protein interaction network. Hub targets of SZDTD in treating allergic asthma were screened by degree values, in which red nodes have higher degree values. The degree value is proportional to the size of the target node. (**D**–**F**) GO analysis of candidate targets, including molecular functions, cellular components, and biological processes. (**G**) KEGG analysis of signaling pathways enriched by candidate genes.

Name	Degree	Betweenness Centrality
AKT1	57	0.220325616
TNF	56	0.184661791
SRC	37	0.052973683
PTGS2	37	0.064848553
EGFR	35	0.039737243
PPARG	34	0.06237236
MMP9	32	0.018936509
ESR1	28	0.049703705
MMP2	23	0.005746224
KDR	23	0.010960582
IL2	22	0.011247008
MPO	20	0.008005159
PPARA	20	0.019267169
CNR1	17	0.054570176
SLC6A4	16	0.064096006
ABCB1	16	0.023526081
PTK2	15	0.006525266
MMP3	15	0.001693134
GSK3B	15	0.003297087
IGF1R	15	0.001359822

Table 1. Genes in the top 20 Degree values.

disassembly. In terms of cellular components (CC), the target genes were associated with integral component of plasma membrane, integral component of presynaptic membrane, plasma membrane, integral component of postsynaptic membrane, and presynaptic membrane. The molecular functions (MF) of the target genes predominantly included serine-type endopeptidase activity, identical protein binding, enzyme binding, oxidoreductase activity with incorporation of molecular oxygen, and endopeptidase activity (Fig. 2D–F). The KEGG enrichment analysis indicated that treatment with SZDTD for allergic asthma primarily influenced pathways related to immune responses, inflammation, cancer, lipid metabolism, and other associated pathways. Notably, with a significance level of $P < 0.05$, immune-related pathways were significantly enriched (Fig. 2G). Among these pathways, the AMPK signaling pathway was identified, involving core genes such as AKT1, PPARG, and IGF1R. Interestingly, these genes were clustered together in the MCODE analysis subset, suggesting a close association between SZDTD and the AMPK and PI3K/AKT signaling pathways.

Identification of active ingredients in SZDTD

To investigate the main components of ethanol extract of SZDTD, the SZDTD was analyzed by UPLC- MS. The results showed main six peaks in positive mode (Fig. 3A) and five peaks in negative mode (Fig. 3B), which were identified as follows: DL-Stachydrine, N-(2,4-Dimethylphenyl)formamide, Naringin, 18-β-Glycyrrhetinic acid, Nobiletin, Tangeritin, D-(-)-Quinic acid, Eriocitrin, Hydroxyferulic acid, apigenin-7-O-glucuronide.

Effect of SZDTD on inflammatory cells in BALF of asthmatic mice

As Fig. 4 shows, the total cell count, eosinophil, lymphocyte, and neutrophil counts were significantly increased in the MOD group compared to the CON group ($P < 0.05$). Conversely, the counts were notably reduced in the treated groups compared to the MOD group ($P < 0.05$).

Effect of SZDTD on cytokines in mouse BALF and serum IgE

According to the ELISA results, the expression levels of IL-4, IL-5, IL-13, serum total IgE, and OVA-specific IgE were significantly elevated in the MOD group compared with the CON group ($P < 0.05$), while IL-4, IL-5, IL-13, and total Ig E and OVA-specific IgE expression levels were significantly lower in the treatment groups compared with the MOD group ($P < 0.05$). This result suggests that SZDTD can attenuate the inflammatory response in OVA mice by reducing Th2-type cytokines (Table 2).

Effect of SZDTD on IL-4 and IFN-γ in spleen and lymph nodes

As shown in Fig. 5A–D, the levels of IFN-γ, which represent Th1-type cytokines, and IL-4, representative of Th2-type cytokines, were significantly increased in the spleens and lymph nodes of mice in the MOD group compared to the CON group, with IL-4 showing a more pronounced increase. Levels of IFN-γ and IL-4 were reduced to varying degrees in the treatment groups compared to the OVA group. Consequently, in the onset and management of OVA-allergic asthma, Th2-type cytokines exhibit greater sensitivity than Th1-type cytokines.

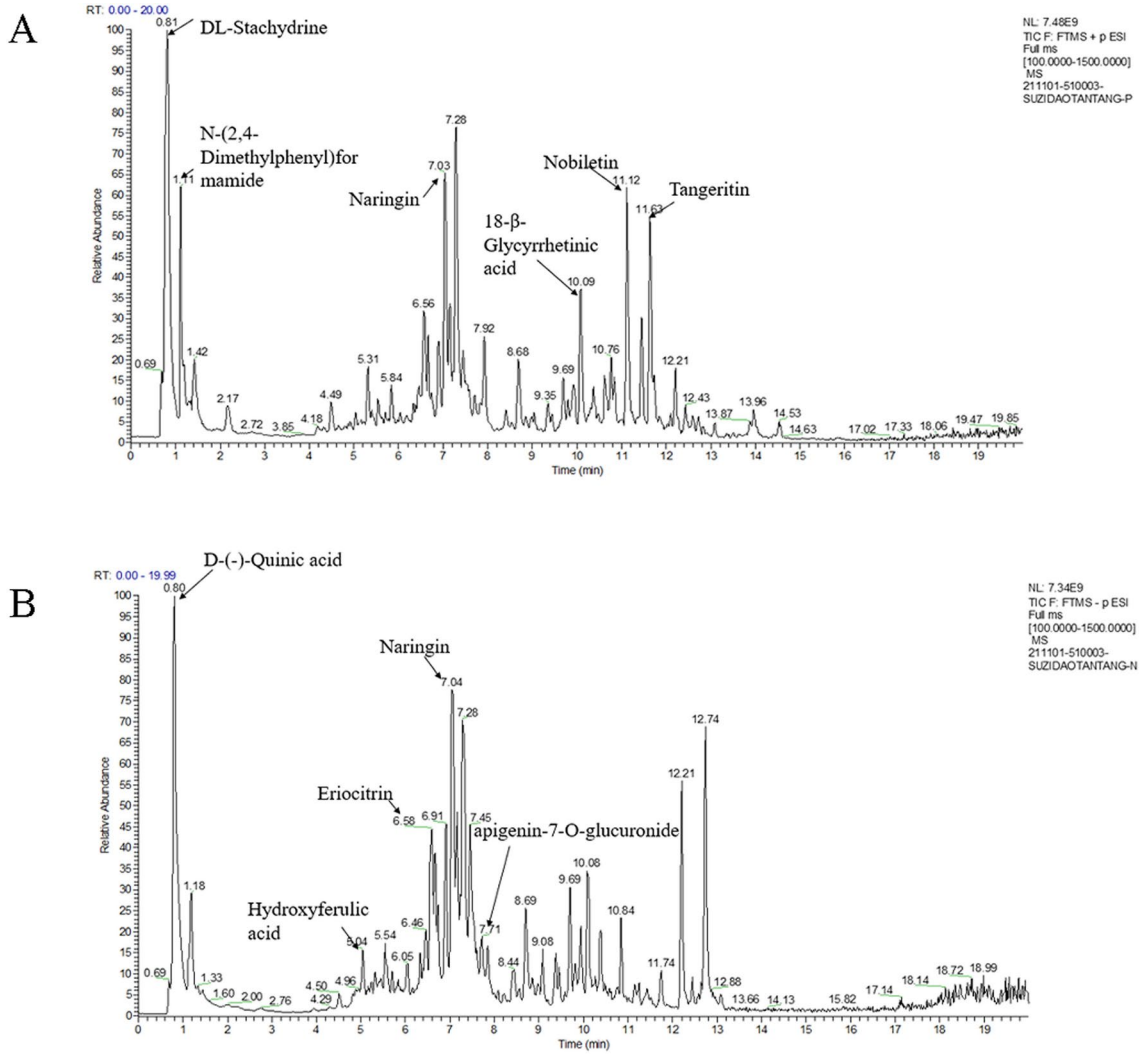

Fig. 3. Chemical profiles of SZDTD by UPLC-Q-TOF MS. (**A**) Positive mode. (**B**) Negative mode. The main components of SZDTD were identified as follows: DL-Stachydrine, N-(2,4-Dimethylphenyl)formamide, Naringin, 18-β-Glycyrrhetinic acid, Nobiletin, Tangeritin, D-(-)-Quinic acid, Eriocitrin, Hydroxyferulic acid, apigenin-7-O-glucuronide.

Effects of SZDTD on histopathological changes in lung tissues

The HE staining results showed (Fig. 6A) that mice in the CON group exhibited normal bronchial and alveolar wall structure, with uniform airway wall thickness and an absence of inflammatory cell infiltration. In contrast, mice in the MOD group displayed noticeable airway wall thickening and damage, along with substantial inflammatory cell infiltration, mucus plug formation, and evident epithelial cell detachment. Compared to the MOD group, SZDTD treatment, particularly in the HIGH group, led to enhancements in airway integrity, reductions in inflammatory cell infiltration, and improvements in airway smooth muscle thickening. The results from MASSON staining (Fig. 6B) indicated minimal collagen fiber deposition around the airways of mice in the CON group. In contrast, a significant increase in collagen fiber deposition was observed in the MOD group, which was subsequently decreased following treatment.

Effect of SZDTD on α-SMA expression

According to the immunohistochemistry results (Fig. 7A), the MOD group had higher levels of α-SMA positive expression than the CON group, with a subsequent decrease observed post-therapy. Furthermore, immunofluorescence (Fig. 7B) demonstrated that following SZDTD treatment, the α-SMA fluorescence intensity was reduced in the MOD group and increased in the MOD group. The findings suggested that SZDTD could lower α-SMA expression.

Effect of SZDTD on AMPK/SIRT1/PGC-1α signaling pathway

IHC results (Fig. 8A, B) showed that the yellow–brown positive signal of P-AMPK and PGC-1α around the trachea was significantly decreased in the MOD group compared with the CON group. In contrast, the positive

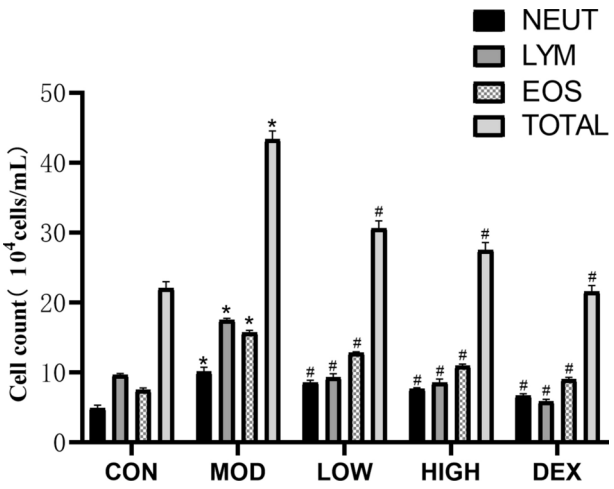

Fig. 4. Effect of SZDTD on the infiltration of inflammatory cells in BALF of allergic asthma mice. The total number of cells in BALF and the number of various inflammatory cells. $^{*}P < 0.05$ vs CON group. $^{\#}P < 0.05$vs MOD group. Data was presented as mean ± SD, n = 10.

Group	IL-4 (pg/mL)	IL-5 (pg/mL)	IL-13 (pg/mL)	Total Ig E (ng/mL)	OVA-specific Ig E (ng/mL)
CON	58.57 ± 6.52	47.31 ± 5.81	24.81 ± 4.02	104.73 ± 8.84	18.35 ± 5.63
MOD	109.38 ± 5.37*	138.69 ± 6.65*	80.93 ± 8.65*	410.82 ± 25.29*	220.63 ± 26.56*
LOW	92.27 ± 5.67#	96.65 ± 4.61#	72.51 ± 5.31#	367.73 ± 19.36#	162.44 ± 18.54#
HIGH	82.31 ± 11.95#	75.13 ± 7.96#	55.43 ± 3.87#	296.39 ± 11.69#	141.47 ± 18.94#
DEX	78.11 ± 3.99#	67.18 ± 7.98#	52.84 ± 4.37#	271.62 ± 23.92#	137.48 ± 15.87#

Table 2. Effect of SZDTD on the levels of relevant cytokines in BALF and immunoglobulins in serum. $^{*}P < 0.05$ vs CON group. $^{\#}P < 0.05$vs MOD group.

signal increased in the treated groups relative to the MOD group. IF analysis (Fig. 8C–E) further revealed a significant reduction in the fluorescence intensity of P-AMPK, SIRT1, and PGC-1α in the MOD group compared to the CON group. Following treatment, the fluorescence intensity increased, particularly in the HIGH group. WB (Fig. 8F, G) revealed a substantial decrease in the protein levels of P-AMPK, SIRT1, and PGC-1α in the MOD group, whereas these levels were significantly increased in the treatment groups, indicating that SZDTD promoted the expression of these proteins. Moreover, MTT assay results demonstrated a significant decrease in cell proliferation ability following LPS stimulation, which notably increased after treatment with SZDTD (Fig. 10A). Thus, concentrations of 12.5, 25, and 50 μg/mL were selected as the low, medium, and high dose groups, respectively. The observed trend of AMPK signaling pathway-related protein expression detected by Western blotting was consistent with the outcomes of the animal experiments (Fig. 10B–C). These results consistently showed that SZDTD alleviated asthma by activating the AMPK/SIRT1/PGC-1α signaling pathway.

Effect of SZDTD on PI3K/AKT signaling pathway

The IHC results (Fig. 9A, B) showed a significant increase in the yellow–brown positive signal of P-PI3K and P-AKT around the trachea in the MOD group compared to the CON group, whereas the positive signal decreased in the treated groups relative to the MOD group. IF results further showed (Fig. 9C, D) a significant increase in the fluorescence intensity of P-PI3K and P-AKT in the MOD group compared to the CON group, with a subsequent decrease in fluorescence intensity observed after treatment. Western blot analysis (Fig. 9E, F) indicated a significant increase in the protein levels of P-PI3K and P-AKT in the MOD group, while the protein levels of P-PI3K and P-AKT were significantly decreased in the treatment groups. The trend of PI3K signaling pathway-related protein expression detected by WB in vitro experiments was consistent with the results of animal experiments (Fig. 10D, E). These results consistently indicated that SZDTD relieved asthma by inhibiting the PI3K/AKT signaling pathway.

Discussion

Asthma, as a heterogeneous disease, exhibits respiratory symptoms and airflow limitation related to airway inflammation and airway remodeling[19]. Airway remodeling is an important mechanism in the pathogenesis of asthma, characterized by epithelial damage and ciliary dysfunction, proliferation of mucous glands, extracellular matrix (ECM) deposition, thickening of the airway reticular layer, regeneration of blood vessels, epithelial

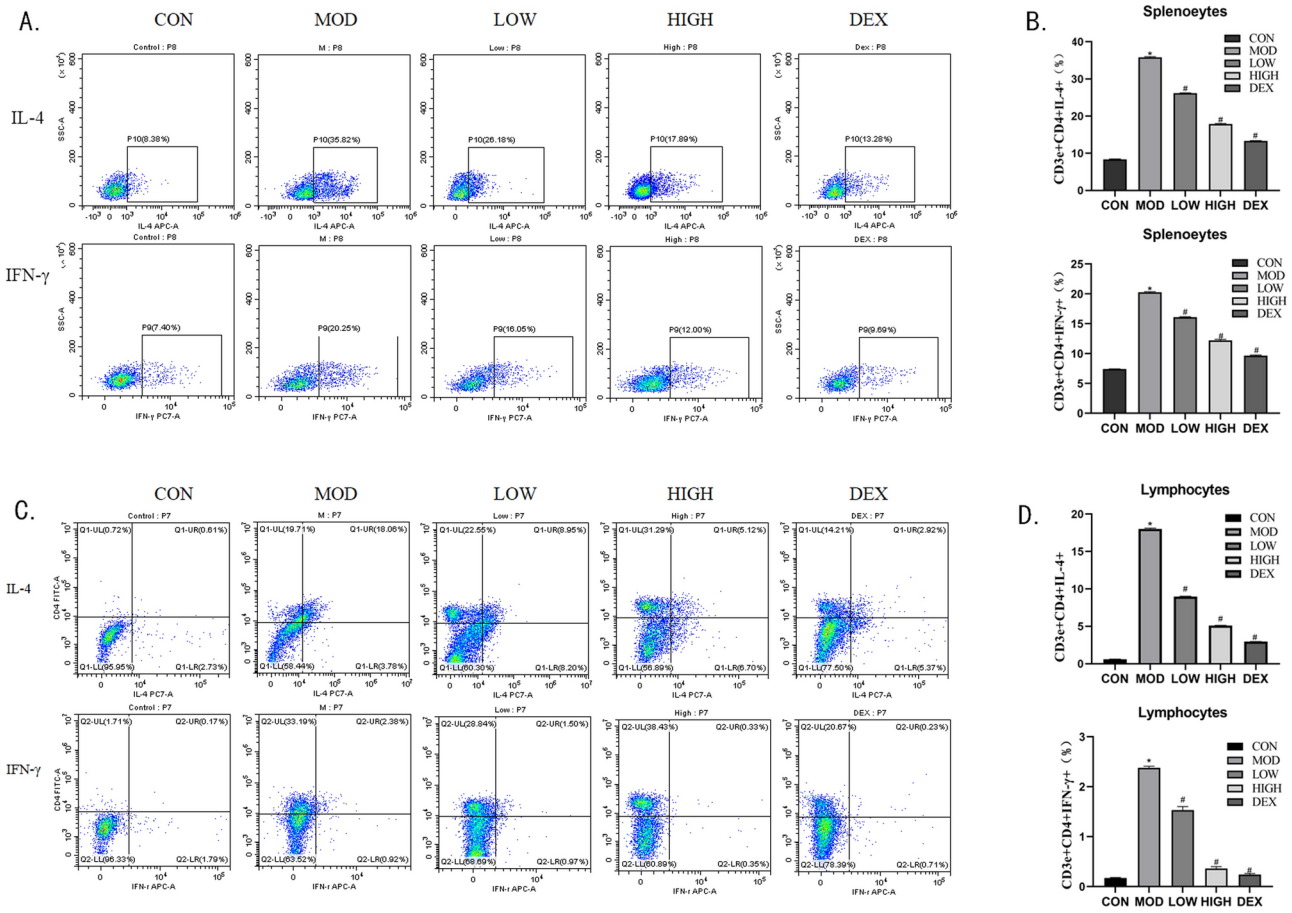

Fig. 5. Effect of SZDTD on the levels of Th1/Th2 cytokines in spleen and lymph node. SZDTD decreases the levels of IL-4 and IFN-γ in the spleen (**A**, **B**) and lymph node (**C**, **D**). $^{*}P < 0.05$ vs CON group. $^{\#}P < 0.05$vs MOD group. Data was presented as mean ± SD, n = 10.

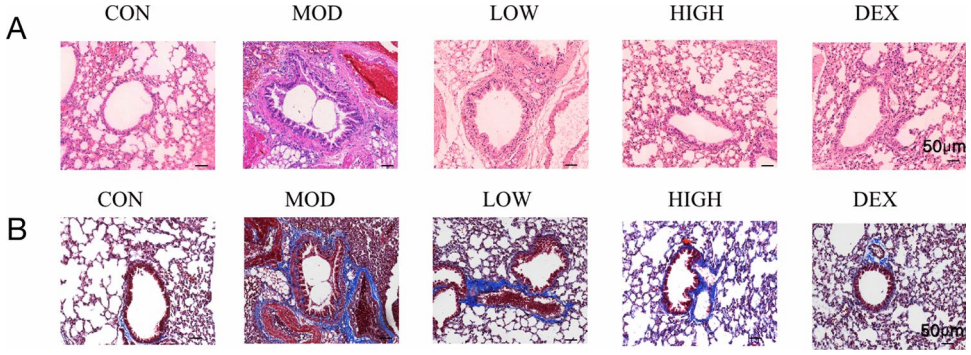

Fig. 6. Effects of SZDTD on histopathological changes in Lung tissues. (**A**) HE staining, scale bar: 50 μm. (**B**) Masson staining, scale bar: 50 μm. n = 10.

fibrosis, and airway smooth muscle cell proliferation and migration[20]. These remodeling features lead to the thickening of the airway wall, impacting quality of life. Studies show higher rates of incomplete asthma control[21].

SZDTD, formulated for individuals with Shao-Yin constitution, exerts efficacy in fortifying the spleen and internal guardianship, regulating qi, and resolving phlegm, thereby demonstrating effectiveness in the management of phlegm asthma. Our research has unveiled that naringin, a key component of SZDTD, mitigates lung tissue pathological damage[22], activates AMPK and PGC-1α signaling pathways[23], and suppresses inflammation and MMPs production[24]. Additionally, DL-Stachydrine inhibits inflammation, reduces oxidative stress, ECM, and autophagy, induces apoptosis, and inhibits cell proliferation, migration, and invasion[25]. Nobiletin[26,27], naringenin[28], and tangeritin[29,30] all inhibit inflammation. Moreover, naringenin plays a role in

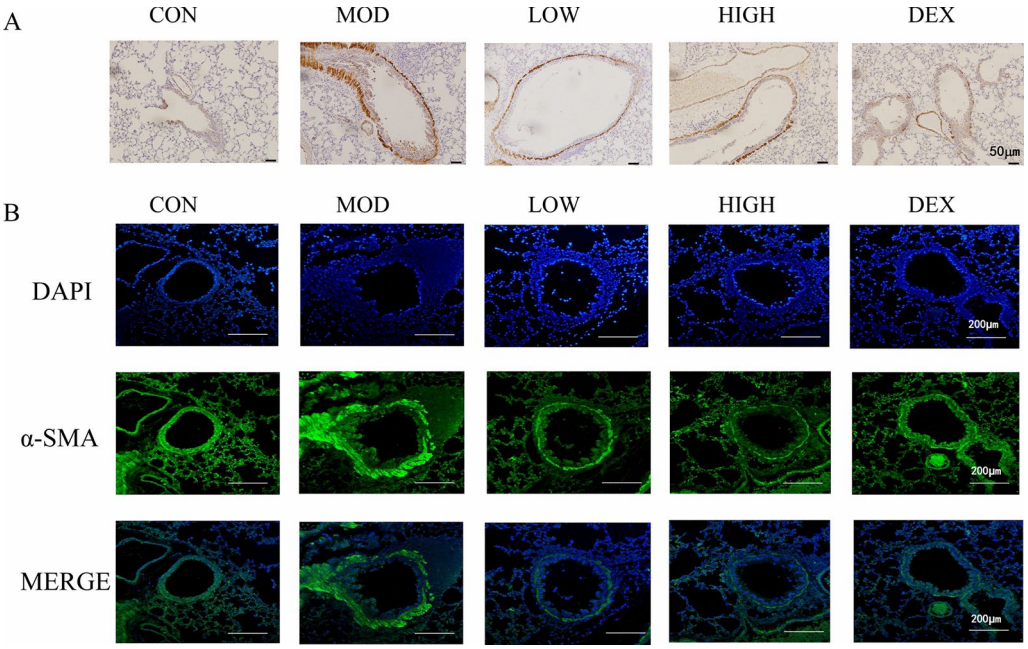

Fig. 7. Effect of SZDTD on α-SMA expression. (**A**) Immunohistochemical staining was performed to detect the expression of α-SMA (scale bar: 50 μm). (**B**) Immunofluorescence assay for α-SMA in the lung sections was performed. (scale bar: 200 μm). Data was presented as mean ± SD, n = 10.

autophagy, while tangeritin exhibits antioxidant properties. 18-β-Glycyrrhetinic acid[31] exerts anti-inflammatory effects by modulating the MAPK/NFκB pathway. Eriocitrin[32] acts as an antioxidant, anti-tumor, anti-allergic, and anti-inflammatory agent, closely linked to the pathogenesis of allergic asthma. Following SZDTD intervention, a significant reduction in inflammatory cell count was observed. α-SMA, which regulates smooth muscle contraction, extracellular matrix deposition, and subepithelial fibrosis in the respiratory system, exhibited decreased expression in lung tissue after SZDTD treatment. These findings underscore the potential of SZDTD in alleviating asthmatic inflammation and airway remodeling.

T helper cells (Th), are closely related to the pathogenesis of asthma, mainly the imbalance between Th1 and Th2 cells[33]. It is well known that Th2 cells produce IL-4, IL-5 and IL-13, and Th1 cells produce IFN-γ[34]. However, the main feature of allergic asthma is the pulmonary infiltration of activated Th2 cells that overexpress cytokines, including IL-4, IL-5, and IL-13, which in turn promotes the activation and infiltration of eosinophils, mast cells, and B lymphocytes[35]. The results demonstrated an elevation in the expression of IL-4, IL-5, and IL-13 post-asthma onset, with alterations in the IL-4, IL-5, and IL-13 ratio contributing to Th1/Th2 imbalance and subsequent IgE release. Results from the current study indicated a notable increase in Th2 cytokines, particularly evident by the flow of spleen and lymph, with a significant elevation in IL-4, a hallmark Th2 cytokine, and a lesser increase in IFN-γ, a Th1 cytokine, compared to IL-4. Both IL-4 and IFN-γ exhibited varying degrees of reduction post-treatment, with IL-4 showing more pronounced changes than IFN-γ. These observations suggest that the mechanism underlying airway remodeling in asthma is linked to Th1/Th2 imbalance, primarily influenced by alterations in the Th2 cell subpopulation. SZDTD exerts its asthma-alleviating effects predominantly through modulation of Th2-type cytokines.

Through enrichment analysis utilizing network pharmacology, we identified a connection between the AMPK signaling pathway, PI3K signaling pathway, and the mechanism of action of SZDTD. AMPK serves as a crucial regulator of energy metabolism and plays a significant role in modulating inflammatory responses and chronic stress. Studies have shown that activation of the AMPK/SIRT1/NF-κB pathway inhibits macrophage polarization towards a pro-inflammatory state[36]. Airway smooth muscle cells (ASMCs) are the main structural cells involved in airway smooth muscle (ASM) remodeling and represent target cells for therapeutic interventions in chronic respiratory conditions like asthma[37]. It was found that activation of AMPK attenuated the TGF-β1-induced proliferation of ASMCs[38]. The team of Jiang[39] and Ma[40] have indicated that airway inflammation and remodeling can be alleviated through AMPK activation. In this study, SZDTD was able to promote the expression of P-AMPK in lung tissue and BEAS-2B human bronchial epithelial cell line, suggesting that SZDTD may activate AMPK to inhibit airway remodeling.

SIRT1, a nicotinamide adenine dinucleotide (NAD+)-dependent protein deacetylase, plays a crucial role in cell cycle regulation, oxidative stress, energy metabolism, and is involved in inflammation and immunity pathways[41]. AMPK transcriptionally activates nicotinamide phosphoribosyltransferase (NAMPT), leading to an increase in the oxidized nicotinamide adenine/reduced nicotinamide adenine dinucleotide (NADH) ratio, subsequently activating SIRT1. The current study revealed that SZDTD induces a dose-dependent stimulation of SIRT1 expression. These results suggest that SZDTD mitigates airway remodeling by activating the AMPK/SIRT1 pathway. Asthma relief has been linked to the regulation of energy metabolism by AMPK/SIRT1[42].

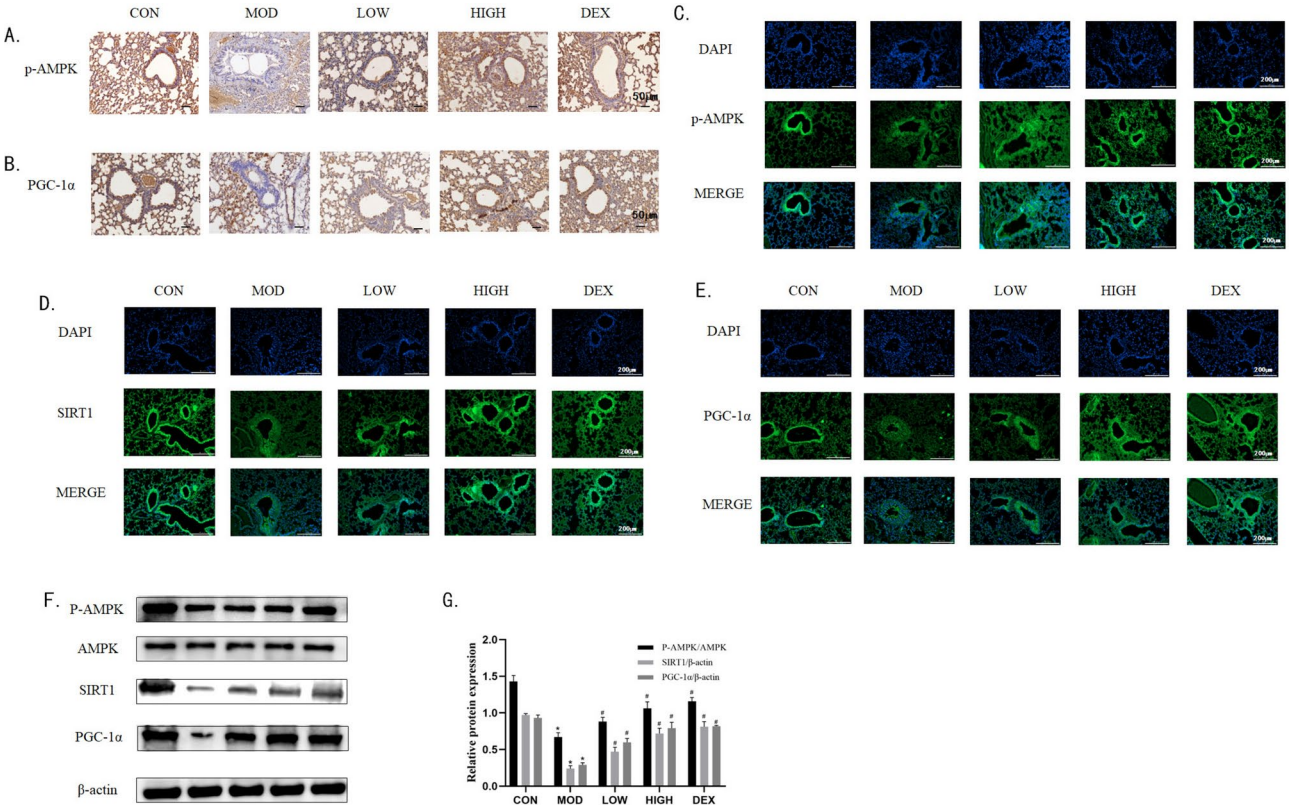

Fig. 8. Effect of SZDTD on AMPK/SIRT1/PGC-1α signaling pathway in mice. (**A**, **B**) Immunohistochemical staining was performed to detect the expression of AMPK and PGC-1α, (scale bar: 50 μm). Immunofluorescence assay for AMPK (**C**), SIRT1 (**D**), PGC-1α (**E**) in the lung sections was performed. (scale bar: 200 μm). (**F**) The production of AMPK, P- AMPK, SIRT1 and PGC-1α in the lung homogenates was estimated by western blotting, and the relative protein expression (**G**) was measured. β-Actin and AMPK are on the same gel, while the rest are on separate gels. $^{*}P < 0.05$ vs CON group. $^{\#}P < 0.05$vs MOD group. Data was presented as mean ± SD, n = 10.

PGC-1α, situated downstream of AMPK and SIRT1, is regulated by the activated AMPK and SIRT1, thereby influencing PGC-1α activity. The AMPK/SIRT1/PGC-1α signaling pathway functions as an energy-sensing network, playing a critical role in mitochondrial biosynthesis, energy metabolism, and oxidative stress regulation[43]. Silencing of PGC-1α exacerbated the increase in TGF-β1 content induced by SiO_2 stimulation, while overexpression of TGF-β1 facilitated fibroblast activation, promoting collagen deposition[44]. Hence, the upregulation of PGC1α expression can mitigate collagen deposition and ameliorate airway remodeling in asthma. WB, IHC, and IF analyses in this study revealed a dose-dependent increase in PGC-1α levels in OVA mice following SZDTD treatment. Furthermore, treatment with SZDTD led to elevated PGC-1α expression in the BEAS-2B human bronchial epithelial cell line. These findings suggest that SZDTD maintains downstream signaling activation post-AMPK activation. Collectively, these results indicate that SZDTD effectively alleviates asthmatic airway remodeling by engaging the AMPK/SIRT1/PGC-1α signaling pathway.

Phosphatidylinositol 3-kinase (PI3K)/protein kinase B (PKB/AKT) signaling pathway serves as a pivotal cellular pathway regulating cell growth, proliferation, motility, metabolism and survival[45]. Studies have indicated that increased expression of α-SMA is linked to the PI3K/AKT pathway[46]. Research in asthma has demonstrated that inhibiting the PI3K/AKT signaling pathway can alleviate airway inflammation and airway remodeling[47,48]. The results obtained through WB, IF and IHC analyses revealed a reduction in the expression of P-PI3K and P-AKT in OVA mice following SZDTD treatment. In vitro experiments demonstrated decreased protein expression of P-PI3K and P-AKT in LPS-stimulated BEAS-2B human bronchial epithelial cell line post-treatment. In conclusion, SZDTD can effectively alleviate asthma by inhibiting the PI3K/AKT signaling pathway.

This study also has certain limitations. The complex composition of SZDTD involves the interplay and mutual regulation of multiple signaling pathways, with only two pathways explored in this experiment. Furthermore, while this study validated the impact of SZDTD on the AMPK/SIRT1/PGC-1α and PI3K/AKT pathways in alleviating asthma, the identification of the specific traditional Chinese medicine components and core ingredients crucial for the therapeutic effects of SZDTD in asthma remains unresolved. Further experimental validation is warranted to address these aspects comprehensively.

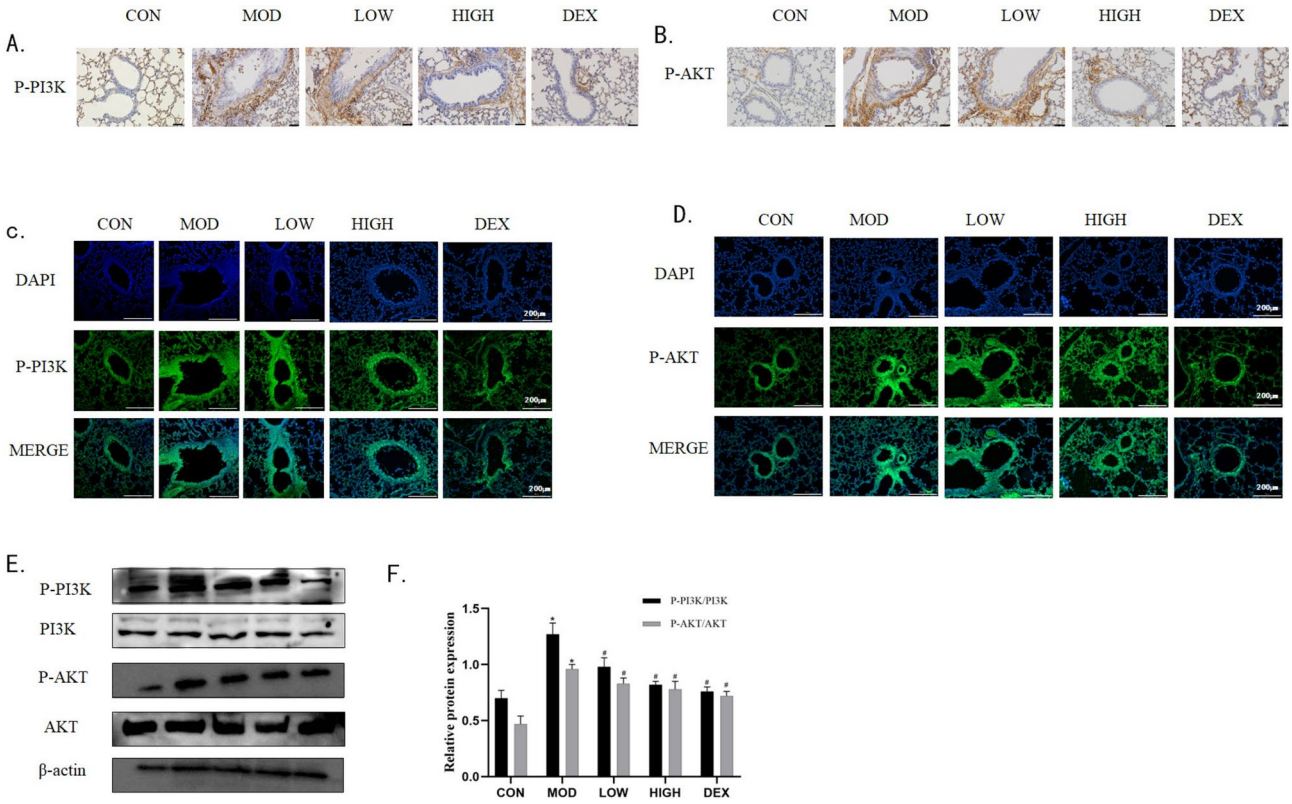

Fig. 9. Effect of SZDTD on PI3K/AKT signaling pathway in mice. (**A**, **B**) Immunohistochemical staining was performed to detect the expression of P-PI3K, P-AKT, (scale bar: 50 μm). Immunofluorescence assay for P-PI3K (**C**), P-AKT (**D**), in the lung sections was performed. (scale bar: 200 μm). (**E**) The production of PI3K, P-PI3K, AKT, P-AKT in the lung homogenates was estimated by western blotting, and the relative protein expression (**F**) was measured. All lanes are separate gels. $^{*}P < 0.05$ vs CON group. $^{\#}P < 0.05$vs MOD group. Data was presented as mean ± SD, n = 10.

Conclusion

The results of this study demonstrated that SZDTD has the effect of alleviating asthmatic airway inflammation and airway remodeling by a mechanism related to the activation of the AMPK/SIRT1/PGC-1α signaling pathway and inhibition of PI3K/AKT signaling pathway. However, further investigation is required to elucidate the precise underlying mechanism.

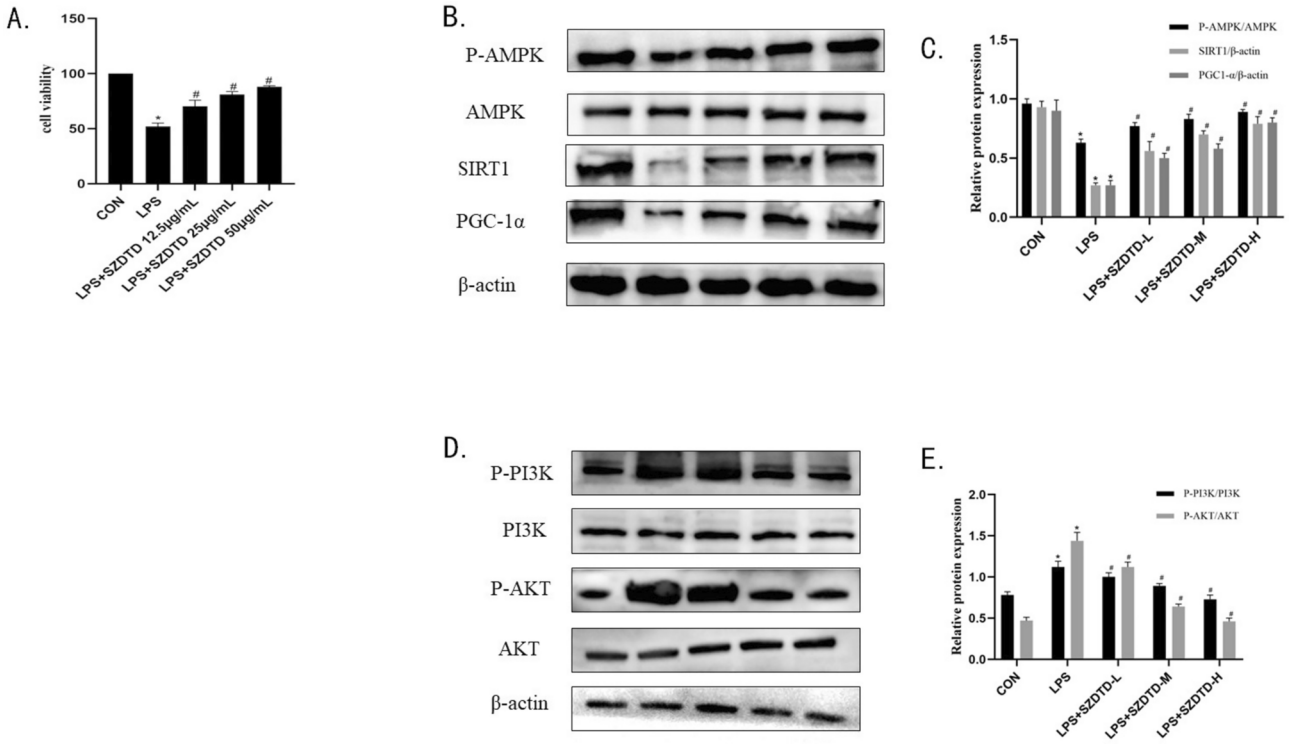

Fig. 10. Effects of SZDTD on AMPK and PI3K signaling pathways in in vitro assays. (**A**) The result of MTT assay to detect the cellular value-added situation. (**B**) The production of AMPK, P- AMPK, SIRT1 and PGC-1α in the BEAS-2B human bronchial epithelial cell line was estimated by western blotting, and the relative protein expression (**C**) was measured. β-Actin and AMPK are on the same gel, P-AMPK and PGC-1α are on the same gel, SIRT1 is on a separate gel. $^{*}P < 0.05$ vs CON group. $^{\#}P < 0.05$vs LPS group. (**D**) The production of PI3K, P-PI3K, AKT, P-AKT in the lung homogenates was estimated by western blotting, and the relative protein expression (**E**) was measured. All lanes are separate gels. $^{*}P < 0.05$ vs CON group. $^{\#}P < 0.05$vs LPS group.

Data availability

Availability of Data and Materials: All data supporting the findings of this study are available within the paper and its Supplementary Information.

Received: 15 December 2024; Accepted: 17 February 2025
Published online: 25 February 2025

References

1. Sockrider, M. & Fussner, L. What is asthma?. *Am J Respir Crit Care Med.* **202**(9), 25–26. https://doi.org/10.1164/rccm.2029P25 (2020).
2. Mims, J. W. Asthma: Definitions and pathophysiology. *Int. Forum Allergy Rhinol.* **5**(Suppl 1), S2–S6. https://doi.org/10.1002/alr.21609 (2015).
3. GBD. 2019 Chronic Respiratory Diseases Collaborators (2023). Global burden of chronic respiratory diseases and risk factors, 1990-2019: an update from the Global Burden of Disease Study 2019. *EClinicalMedicine*, **59**, 101936. https://doi.org/10.1016/j.eclinm.2023.101936.
4. Wieczfinska, J. & Pawliczak, R. Anti-fibrotic effect of ciglitazone in HRV-induced airway remodelling cell model. *J. Cell Mol. Med.* **27**(13), 1867–1879. (2023).
5. Guida, G. & Riccio, A. M. Immune induction of airway remodeling. *Semin. Immunol.* **46**, 101346 (2019).
6. Liu, R. The effect of Suzidaotan Decoction, a Traditional Chinese Korean medicine prescription, on airway remodeling in asthmatic mice through wnt5a signaling pathway. Yanbian University. https://kns-cnki-net-443.webvpn.ybu.edu.cn/kcms2/article/(2022).
7. Ru, J. et al. TCMSP: A database of systems pharmacology for drug discovery from herbal medicines. *J. Cheminform.* **6**, 13. https://doi.org/10.1186/1758-2946-6-13 (2014).
8. Xiang, C. et al. Network pharmacology and molecular docking to elucidate the potential mechanism of Ligusticum Chuanxiong against osteoarthritis. *Front. Pharmacol.* **13**, 854215. https://doi.org/10.3389/fphar.2022.854215 (2022).
9. Fang, S. et al. HERB: a high-throughput experiment- and reference-guided database of traditional Chinese medicine. *Nucleic Acids Res.* **49**(D1), D1197–D1206. https://doi.org/10.1093/nar/gkaa1063 (2021).
10. Kim, S. et al. PubChem in 2021: New data content and improved web interfaces. *Nucleic Acids Res.* **49**(D1), D1388–D1395. https://doi.org/10.1093/nar/gkaa971 (2021).
11. Lipinski, C. A., Lombardo, F., Dominy, B. W. & Feeney, P. J. Experimental and computational approaches to estimate solubility and permeability in drug discovery and development settings. *Adv. Drug Deliv. Rev.* **46**(1–3), 3–26. https://doi.org/10.1016/s0169-409x(00)00129-0 (2001).
12. Gfeller, D., Grosdidier, A., Wirth, M., Daina, A., Michielin, O., Zoete, V. SwissTargetPrediction: A web server for target prediction of bioactive small molecules. *Nucleic Acids Res.*, **42**(Web Server issue), W32–W38. https://doi.org/10.1093/nar/gku293(2014).

13. Hu, Y. et al. Mechanism of Marsdenia tenacissima against ovarian cancer based on network pharmacology and experimental verification. *China J. Chin. Materia Med.* **48**(08), 2222–2232. https://doi.org/10.19540/j.cnki.cjcmm.20230103.704 (2023).
14. Szklarczyk, D. et al. The STRING database in 2021: Customizable protein-protein networks, and functional characterization of user-uploaded gene/measurement sets. *Nucleic Acids Res.* **49**(D1), D605–D612. https://doi.org/10.1093/nar/gkaa1074 (2021).
15. Shannon, P. et al. Cytoscape: A software environment for integrated models of biomolecular interaction networks. *Genome Res.* **13**(11), 2498–2504. https://doi.org/10.1101/gr.1239303 (2003).
16. Dennis, G. Jr. et al. DAVID: Database for annotation, visualization, and integrated discovery. *Genome Biol.* **4**(5), P3 (2003).
17. Song, Y. et al. DEK-targeting aptamer DTA-64 attenuates bronchial EMT-mediated airway remodelling by suppressing TGF-β1/Smad, MAPK and PI3K signalling pathway in asthma. *J. Cell Mol. Med.* **24**(23), 13739–13750. https://doi.org/10.1111/jcmm.15942 (2020).
18. Bao, H. R., Liu, X. J., Li, Y. L., Men, X. & Zeng, X. L. Sinomenine attenuates airway inflammation and remodeling in a mouse model of asthma. *Mol. Med. Rep.* **13**(3), 2415–2422. https://doi.org/10.3892/mmr.2016.4816 (2016).
19. Papi, A., Brightling, C., Pedersen, S. E. & Reddel, H. K. Asthma. *Lancet (London, England)* **391**(10122), 783–800. https://doi.org/10.1016/S0140-6736(17)33311-1 (2018).
20. Banno, A., Reddy, A. T., Lakshmi, S. P., Reddy, R. C. Bidirectional interaction of airway epithelial remodeling and inflammation in asthma. *Clin. Sci.* (London, England: 1979), **134**(9), 1063–1079. https://doi.org/10.1042/CS20191309(2020).
21. Wang, J. Analysis of the current status of disease control and its related risk factors in patients with bronchial asthma. *Shanxi Med. J.* **52**(13), 980–982 (2023).
22. Zhang, H. H. et al. Naringin suppressed airway inflammation and ameliorated pulmonary endothelial hyperpermeability by upregulating Aquaporin1 in lipopolysaccharide/cigarette smoke-induced mice. *Biomed. Pharmacother.* **150**, 113035. https://doi.org/10.1016/j.biopha.2022.113035 (2022).
23. Li, P. et al. Naringin promotes skeletal muscle fiber remodeling by the AdipoR1-APPL1-AMPK signaling pathway. *J. Agric. Food Chem.* **69**(40), 11890–11899. https://doi.org/10.1021/acs.jafc.1c04481 (2021).
24. Aihaiti, Y. et al. Therapeutic effects of naringin in rheumatoid arthritis: network pharmacology and experimental validation. *Front. Pharmacol.* **12**, 672054. https://doi.org/10.3389/fphar.2021.672054 (2021).
25. Cheng, F. et al. A review of pharmacological and pharmacokinetic properties of stachydrine. *Pharmacol. Res.* **155**, 104755. https://doi.org/10.1016/j.phrs.2020.104755 (2020).
26. Yang, X., Deng, Y., Tu, Y., Feng, D. & Liao, W. Nobiletin mitigates NAFLD via lipophagy and inflammation. *Food Funct.* **13**(19), 10186–10199. https://doi.org/10.1039/d2fo01682f (2022).
27. Rong, X. et al. Citrus peel flavonoid nobiletin alleviates lipopolysaccharide-induced inflammation by activating IL-6/STAT3/FOXO3a-mediated autophagy. *Food Funct.* **12**(3), 1305–1317. https://doi.org/10.1039/d0fo02141e (2021).
28. Stabrauskiene, J., Kopustinskiene, D. M., Lazauskas, R. & Bernatoniene, J. Naringin and Naringenin: Their mechanisms of action and the potential anticancer activities. *Biomedicines* **10**(7), 1686. https://doi.org/10.3390/biomedicines10071686 (2022).
29. Singh, B., Singh, J. P., Kaur, A., Singh, N. Phenolic composition, antioxidant potential and health benefits of citrus peel. *Food Res. Int. (Ottawa, Ont.)*, **132**, 109114. https://doi.org/10.1016/j.foodres.2020.109114(2020).
30. Shi, Y. et al. Tangeretin suppresses osteoarthritis progression via the Nrf2/NF-κB and MAPK/NF-κB signaling pathways. *Phytomed.: Int. J. Phytother. Phytopharmacol.* **98**, 153928. https://doi.org/10.1016/j.phymed.2022.153928 (2022).
31. Feng, Y., Mei, L., Wang, M., Huang, Q. & Huang, R. Anti-inflammatory and pro-apoptotic effects of 18beta-glycyrrhetinic acid in vitro and in vivo models of rheumatoid arthritis. *Front. Pharmacol.* **12**, 681525. https://doi.org/10.3389/fphar.2021.681525 (2021).
32. Yao, L., Liu, W., Bashir, M., Nisar, M. F., Wan, C. C. Eriocitrin: A review of pharmacological effects. Biomed. Pharmacother. **154**, 113563. https://doi.org/10.1016/j.biopha.2022.113563(2022).
33. Gans, M. D. & Gavrilova, T. Understanding the immunology of asthma: Pathophysiology, biomarkers, and treatments for asthma endotypes. *Paediatr. Respir. Rev.* **36**, 118–127. https://doi.org/10.1016/j.prrv.2019.08.002 (2020).
34. Agache, I., Palmer, E., Sanver, D., Kirtland, M. & Shamji, M. H. Molecular allergology approach to allergic asthma. *Mol. Aspects Med.* **85**, 101027. https://doi.org/10.1016/j.mam.2021.101027 (2022).
35. Asayama, K. et al. Protein S protects against allergic bronchial asthma by modulating Th1/Th2 balance. *Allergy* **75**(9), 2267–2278. https://doi.org/10.1111/all.14261 (2020).
36. Ye, Q. et al. Apoptotic extracellular vesicles alleviate Pg-LPS induced inflammatory responses of macrophages via AMPK/SIRT1/NF-κB pathway and inhibit osteoclast formation. *J. Periodontol.* **93**(11), 1738–1751. https://doi.org/10.1002/JPER.21-0657 (2022).
37. Lei, J., Zhu, H., Xiao, Y., Li, Y. & Zhao, L. The role of AMPK in bronchial asthma and its research progress. *Chin. J. Respir. Crit. Care Med.* **21**(12), 93–898 (2022).
38. Pan, Y. et al. Activation of AMPK suppresses S1P-induced airway smooth muscle cells proliferation and its potential mechanisms. *Mol. Immunol.* **128**, 106–115. https://doi.org/10.1016/j.molimm.2020.09.020 (2020).
39. Jiang, T., Zhao, D., Zheng, Z. & Li, Z. Sigma-1 receptor alleviates airway inflammation and airway remodeling through AMPK/CXCR4 signal pathway. *Inflammation* **45**(3), 1298–1312. https://doi.org/10.1007/s10753-022-01621-4 (2022).
40. Ma, W. et al. Metformin ameliorates inflammation and airway remodeling of experimental allergic asthma in mice by restoring AMPKα activity. *Front. Pharmacol.* **13**, 780148. https://doi.org/10.3389/fphar.2022.780148 (2022).
41. Zheng, Z., Bian, Y., Zhang, Y., Ren, G. & Li, G. Metformin activates AMPK/SIRT1/NF-κB pathway and induces mitochondrial dysfunction to drive caspase3/GSDME-mediated cancer cell pyroptosis. *Cell Cycle* **19**(10), 1089–1104. https://doi.org/10.1080/15384101.2020.1743911 (2020).
42. Xu, C. et al. Pterostilbene suppresses oxidative stress and allergic airway inflammation through AMPK/Sirt1 and Nrf2/HO-1 pathways. *Immunity Inflam. Dis.* **9**(4), 1406–1417. https://doi.org/10.1002/iid3.490 (2021).
43. Cantó, C. & Auwerx, J. PGC-1alpha, SIRT1 and AMPK, an energy sensing network that controls energy expenditure. *Curr. Opin. Lipidol.* **20**(2), 98–105. https://doi.org/10.1097/MOL.0b013e328328d0a4 (2009).
44. He, H. et al. Regulation of PGC1a on SiO_2-induced lipid accumulation in macrophages and fibrosis in pulmonary fibroblasts. *J. Environ. Occup. Med.* **40**(10), 1201–1206 (2023).
45. Yang, J. et al. Targeting PI3K in cancer: Mechanisms and advances in clinical trials. *Mol Cancer* **18**(1), 26. https://doi.org/10.1186/s12943-019-0954-x (2019).
46. Huang, W. et al. Emodin ameliorates myocardial fibrosis in mice by inactivating the ROS/PI3K/Akt/mTOR axis. *Clin Exp Hypertens* **46**(1), 2326022. https://doi.org/10.1080/10641963.2024.2326022 (2024).
47. Peng, W. et al. FGF10 attenuates allergic airway inflammation in asthma by inhibiting PI3K/AKT/NF-κB pathway. *Cell Signal.* **113**, 110964. https://doi.org/10.1016/j.cellsig.2023.110964 (2024).
48. Liu, J., Li, L., Han, X., Chen, Y. & Diao, J. Loke zupa decoction attenuates bronchial EMT-mediated airway remodelling in chronic asthma through the PI3K-Akt/HIF-1α signaling pathway. *Pharm Biol.* **61**(1), 1332–1342. https://doi.org/10.1080/13880209.2023.2244543 (2023).

Author contributions

Kaiyue Liu contributed to the design of the work, acquisition, analysis, inter-pretation of data, draft the work and substantively revise it. Ruobai Liu contributed to the design of the work, acquisition, analysis, interpretation of data, and substan-tively revise it. Chenghao Zhang contributed to the acquisition, analysis, interpreta-tion of data, and substantively revise it. Dandan Huang and Bowen Wei contributed to the acquisition, analysis of data.

Yilan Song and Chongyang Wang contributed to the design of the work, analysis, interpretation of data. Xin Zhang contributed to the analysis of data. Mingyu Zheng and Guanghai Yan contributed to the concep-tion, design of the work and substantively revised it. All authors have read and agreed to the published version of the manuscript.

Funding
This work was supported by the National Natural Science Foundation of China (Nos. 82060911, 81970018). The funder had no role in the design of the study; in the collection, analysis, or interpretation of data; in the writing of the manuscript; or in the decision to publish the results.

Declarations

Ethics approval and consent to participate
This study was approved by the Institutional Animal Care and Use Committee of Yanbian University (IACUC Issue No. YD20230711001).

Statements related to the ARRIVE guidelines
The experimental procedure of this study was in accordance with ARRIVE guidelines.

Consent for publication
All authors have read and agreed to the published version of the manuscript.

Competing interests
The authors declare no competing interests.

Additional information
Supplementary Information The online version contains supplementary material available at https://doi.org/10.1038/s41598-025-90870-y.

Correspondence and requests for materials should be addressed to M.Z. or G.Y.

Reprints and permissions information is available at www.nature.com/reprints.

Publisher's note Springer Nature remains neutral with regard to jurisdictional claims in published maps and institutional affiliations.